Macromolecules

ARTICLE

pubs.acs.org/Macromolecules

Charge Inversion by Flexible Polyelectrolytes on Spherical Surfaces: Numerical Self-Consistent Field Calculations under the Ground-State Dominance Approximation

Zhengjia Wang, Baohui Li,* and Datong Ding

School of Physics and Key Laboratory of Functional Polymer Materials of Ministry of Education, Nankai University, Tianjin 300071, China

Qiang Wang*

Department of Chemical and Biological Engineering, Colorado State University, Fort Collins, Colorado 80523-1370, United States

ABSTRACT: The adsorption and charge inversion by flexible polyelectrolytes (PEs) onto an oppositely charged spherical surface from a bulk solution of finite PE concentration are studied via numerically solving the coupled ordinary differential equations derived from the continuum self-consistent field (SCF) theory under the ground-state dominance approximation. The effects of various parameters, including the particle radius (r_0) and its surface charge density (σ_{sf}), PE charge fraction (p), short-range surface−PE interaction, solvent quality, and bulk PE concentration and salt concentration, on the amount of adsorbed PEs (Γ) and charge inversion ratio are investigated in detail. It is found that in salt-free solutions where the electrostatic interaction is dominant a relationship of $\Gamma \approx \sigma_{sf} r_0^2/p$ is generally satisfied. The critical particle radius and its surface charge density for PE adsorption are computed as a function of the bulk salt concentration. It is also found that PE adsorption occurs in most cases, whereas strong charge inversion cannot occur either in salt-free solutions or for nonadsorbing surfaces. For attractive surfaces, increasing the bulk salt concentration, or decreasing the surface charge density and the particle radius, generally enhances the charge inversion. Our results on the charge inversion are consistent with previous SCF calculations for planar and cylindrical surfaces.

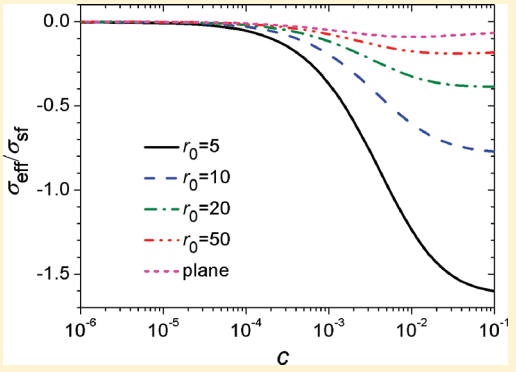

1. INTRODUCTION

The interaction of polyelectrolytes (PEs) with oppositely charged particles is relevant to numerous industrial applications, such as paper making,[1] water treatment,[2] food technology,[3] and powder processing.[4] In addition, the adsorption of PEs onto charged surfaces is a fundamental process in biological systems[5−7] and has been the subject of extensive research in recent years. The critical conditions at which crossover between PE adsorption and desorption occurs depend on the charge density of the surface, the quality of the solvent, the concentrations of salt and PEs in the solution, etc.[8] Since the surface charge inversion is due to PE adsorption, these parameters affect the surface charge inversion phenomenon as well. In some cases, surface geometry also plays an important role in PE adsorption and charge inversion.

A few years ago, one of us applied a continuum self-consistent field (SCF) theory to flexible PEs on planar surfaces and used the ground-state dominance approximation (GSDA) to explore the large parameter space involved, including the PE charge distribution and degree of ionization, surface charge density, short-range (non-Coulombic) surface−polymer interactions, solvent quality, and bulk polymer and salt concentrations; strong charge inversion was found for relatively long polyelectrolytes on oppositely charged, attractive surfaces in poor solvent at high salt concentrations.[9] Following that work, here we study the adsorption and charge inversion of flexible PEs on oppositely charged spherical surfaces by numerically solving the SCF equations under GSDA, which consist of two coupled ordinary differential equations (ODEs): a GSDA equation for the polymer segmental density $\phi_p(r)$ and a Poisson−Boltzmann (PB) equation for the electrostatic potential $\psi(r)$, where r denotes the radial distance from the center of the spherical particle; see eqs 1 and 2 below.

The corresponding ODEs for an implicit good or Θ solvent have been studied by several groups in the past. Von Goeler and Muthukumar,[10] Haronska et al.,[11] and Winkler and Cherstvy[8,12−14] replaced the PB equation with the screened Coulomb potential between PE segments and the spherical surface in the GSDA equation and reported under further

Received: July 15, 2011
Revised: September 30, 2011
Published: October 18, 2011

approximations analytical solutions to the latter with $\lambda_0 = 0$ defining the critical condition for PE adsorption (i.e., the crossover between PE adsorption and desorption) and the boundary conditions of $\phi_p(r=r_0) = \phi_p(r\rightarrow\infty) = 0$, where r_0 denotes the radius of the spherical particle. In addition, Gurovitch and Sens considered the problem of charge inversion in the case of a pointlike particle ($r_0 = 0$) with $\phi_p(r\rightarrow\infty) = 0$, no small ions, and no excluded-volume interactions; $\psi(r)$ can therefore be solved from eq 2 in terms of $\phi_p(r)$, and the corresponding eq 1 for an implicit Θ solvent was then solved analytically by an approximate variational approach.[15] Golestanian, however, showed that the result depends crucially on the choice of the trial function.[16] Finally, Allen and Warren numerically solved the coupled ODEs with two different boundary conditions of $\phi_p(r=r_0) = 0$ and $d\phi_p/dr|_{r=r_0} = 0$ to study the phase behavior of oppositely charged PE−macroion systems with a spherical cell model of finite radius corresponding to the concentration of spherical particles (macroions),[17,18] and similar work was briefly reported by Cherstvy and Winkler for the case of an implicit Θ solvent and $d\phi_p/dr|_{r=r_0} = 0$.[12]

In this work, we study the PE adsorption onto a single spherical particle from a bulk solution of finite PE segmental density (i.e., $\phi_{pb} > 0$) and the related surface charge inversion by numerically solving the coupled ODEs. As in ref 9, we treat the small ions and solvent molecules explicitly and explore the large (seven-dimensional) parameter space involved, including the PE degree of ionization, particle radius and its surface charge density, short-range (non-Coulombic) surface−polymer interactions, solvent quality, and bulk polymer and salt concentrations. One thing to note is that, while more experimentally relevant than $\phi_{pb} = 0$, the finite $\phi_{pb} > 0$ used here makes our definition of the critical condition for PE adsorption different from (thus not directly comparable to) the previous analytical work,[8,10−14] as explained in detail in section 2.

2. THEORETICAL FORMALISM

In this work, we consider a model system that contains a spherical particle of radius r_0 and charged homopolymers, along with added salt and counterions from the polymers and particle, in a solution of small-molecule solvent. We only consider systems with monovalent added salt, in equilibrium with a bulk solution. Without loss of generality, we set the particle surface to be positively charged with a uniform surface charge density σ_{sf}, and each polymer segment carries the same fraction p of an electron charge. We assume that the system has a spherical symmetry and take the center of the particle as $r = 0$. The inside of the particle is not considered and the radius of our system is denoted by L (taken to be large enough as explained below), so that the volume of our system is $V = 4\pi(L^3 - r_0^3)/3$. We assume that both polymer segments and solvent molecules have the same bulk number density ρ_0, ignore the volume of small ions, and impose the incompressibility constraint that requires the total number density of polymer segments and solvent molecules be ρ_0 everywhere in the system. All quantities used in this paper are normalized and dimensionless: All lengths are in units of the polymer statistical segment length a; we use a uniform dielectric constant ε in units of e^2/ak_BT, where k_B is the Boltzmann constant, T the absolute temperature, and e the elementary charge; σ_{sf} is in units of e/a^2; and the PE segmental density ϕ_{pb} and the salt concentration c in the bulk solution are in units of ρ_0.

The general formalism of the continuum SCF theory of PEs has been derived by Shi and Noolandi[19] and Wang et al.[20,21] For our system with spherical symmetry, under GSDA the SCF equations are reduced to two coupled ODEs:[9]

$$\frac{d^2\sqrt{\phi_p(r)}}{dr^2} + \frac{2}{r}\frac{d\sqrt{\phi_p(r)}}{dr} - 6[\chi(1-2\phi_p(r)) - \ln(1-\phi_p(r)) - p\psi(r)]\sqrt{\phi_p(r)} = -\lambda_0\sqrt{\phi_p(r)} \quad (1)$$

$$\frac{d^2\psi(r)}{dr^2} + \frac{2}{r}\frac{d\psi(r)}{dr} + \frac{c}{\varepsilon}(e^{-\psi(r)} - e^{\psi(r)}) - \frac{p}{\varepsilon}(\phi_p(r) - \phi_{pb}e^{-\psi(r)}) = 0 \quad (2)$$

where $\phi_p(r)$ denotes the normalized (by ρ_0) PE segmental density (volume fraction) field; the Flory−Huggins parameter χ denotes the short-range interactions between PE segments and solvent molecules; $\psi(r)$ is the electrostatic potential in units of k_BT/e, which is set to zero in the bulk solution; and λ_0 denotes the eigenvalue of the ground state.

At $r = r_0$, we use the following boundary condition for $\phi_p(r)$[9,22]

$$\frac{1}{\sqrt{\phi_p}}\frac{d\sqrt{\phi_p}}{dr}\bigg|_{r=r_0} = d^{-1} \quad (3)$$

where d^{-1} is related to the short-range (van der Waals) interaction between the particle surface and PEs: a surface with $d^{-1} < 0$ is referred to as an attractive surface, that with $d^{-1} > 0$ as a repulsive surface, and that with $d^{-1} = 0$ as an indifferent surface. The limiting case of $d^{-1} \rightarrow \infty$ is referred to as a nonadsorbing surface, where ϕ_p must vanish. We also use the following boundary condition for $\psi(r)$: $d\psi/dr|_{r=r_0} = -\sigma_{sf}/\varepsilon$. At $r = L$ ($\rightarrow\infty$), we use $d\phi_p^{1/2}/dr|_{r=L} = 0$ and $d\psi/dr|_{r=L} = 0$ as the boundary conditions. In all of our calculations we take L to be large enough (in the range of 420−1200) so that both $|\phi_p(r=L) - \phi_{pb}|$ and $|\psi(r=L)|$ are less than 10^{-10}. This effectively represents an infinitely large system and is different from refs 12, 17, and 18 where a finite spherical cell was used corresponding to a finite concentration of spherical particles. We numerically solve the coupled ODEs using a relaxation method[23] to obtain $\phi_p(r)$ and $\psi(r)$.

With the above boundary conditions at $r\rightarrow\infty$, we obtain from eq 1

$$\lambda_0 = 6\chi(1-2\phi_{pb}) - 6\ln(1-\phi_{pb}) \quad (4)$$

for $\phi_{pb} > 0$. In this work we vary ϕ_{pb} from 10^{-5} to 10^{-3}, which gives $\lambda_0 > 0$ for any $\chi \geq 0$. We therefore cannot use $\lambda_0 = 0$ as the critical condition for PE adsorption, in contrast to the previous analytical work where the case of $\phi_{pb} = 0$ was studied.[8,10−14] Instead, we use the amount of adsorbed PEs as the criterion for adsorption/desorption,[9] which is defined as

$$\Gamma = \int_{r_0}^{L}(\phi_p(r) - \phi_{pb})r^2\,dr \quad (5)$$

PEs are depleted from the surface when $\Gamma < 0$, and adsorbed when $\Gamma > 0$. We also calculate the effective surface charge density compensated by the adsorbed PEs, given by

$$\sigma_{eff} = \sigma_{sf} - \frac{p\Gamma}{r_0^2} \quad (6)$$

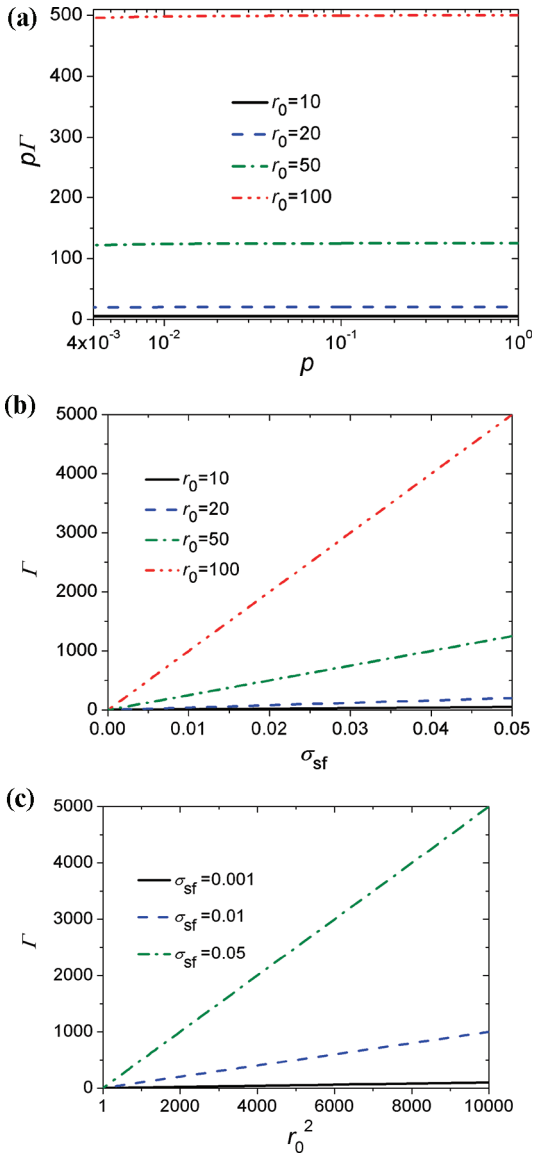

Figure 1. Effects of the PE charge fraction (p), the surface charge density (σ_{sf}), and the particle radius (r_0) on the amount of adsorbed PEs (Γ) for nonadsorbing surface ($d^{-1} \rightarrow \infty$) in the salt-free ($c = 0$) and good solvent ($\chi = 0$) condition. The parameters are $\phi_{pb} = 1.25 \times 10^{-4}$, $\sigma_{sf} = 0.05$ in (a), and $p = 0.1$ in (b) and (c).

The exact charge compensation occurs when $\sigma_{eff} = 0$, charge inversion occurs when $\sigma_{eff} < 0$, and strong charge inversion is obtained when $\sigma_{eff}/\sigma_{sf} \leq -1$. We note that the case of $\phi_{pb} > 0$ is more relevant to experimental systems than that of $\phi_{pb} = 0$, and that for the latter case a numerical problem is also encountered as shown in Figure 4 of ref 9.

3. RESULTS AND DISCUSSION

In this work, we set $a = 0.5$ nm, $T = 300$ K, and $\varepsilon = 0.057$ (corresponding to a dielectric constant of 80). With $\rho_0 = a^{-3}$, $\phi_{pb} = 10^{-4}$ corresponds to a bulk polymer segmental density of about 1.33 mM, $c = 0.015$ corresponds to a bulk salt concentration of about 0.2 M, and $\sigma_{sf} = 0.05$ corresponds to a surface charge density of about 3.26×10^{-2} C/m^2.

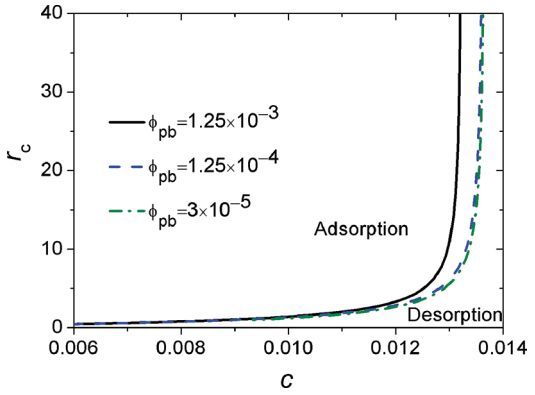

Figure 2. Critical particle radius r_c as a function of the bulk salt concentration c for $\sigma_{sf} = 0.05$, $p = 0.1$, $\chi = 0$, and $d^{-1} \rightarrow \infty$. For the planar surface (i.e., in the limit of $r_c \rightarrow \infty$), the critical values of c are 0.013 23, 0.013 63, and 0.013 66 for $\phi_{pb} = 1.25 \times 10^{-3}$, 1.25×10^{-4}, and 3×10^{-5}, respectively.

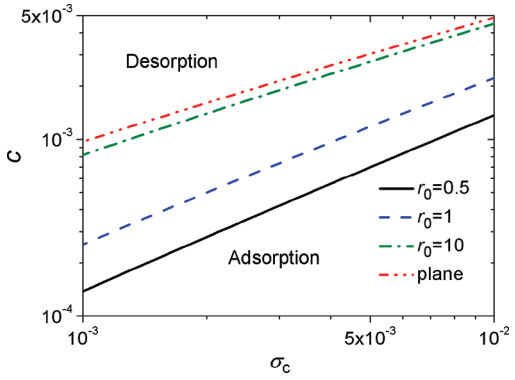

Figure 3. Logarithmic plot of the adsorption−desorption crossover for $p = 0.1$, $\phi_{pb} = 1.25 \times 10^{-4}$, $\chi = 0$, and $d^{-1} \rightarrow \infty$.

3.1. Nonadsorbing Surfaces. In this subsection, unless otherwise specified, we set $d^{-1} \rightarrow \infty$ (corresponding to a nonadsorbing surface) and examine the effects of other parameters on the amount of adsorbed PEs (Γ) and the charge inversion ratio (σ_{eff}/σ_{sf}). Using the scaling argument, Shafir et al.[24] obtained a relationship of $\gamma \approx \sigma_{sf}/p$ for PE adsorption onto charged nonadsorbing planar surfaces under the salt-free condition, where γ denotes the amount of adsorbed PEs per surface area. In the following, we will see that this relationship is applicable to our spherical system as well. Figure 1 shows the effects of PE charge fraction (p), the surface charge density (σ_{sf}), and the particle radius (r_0) on Γ under the salt-free condition in a good solvent ($\chi = 0$); we see from Figure 1a that at given r_0 and σ_{sf} the product of p and Γ is nearly constant, from Figure 1b that at given p and r_0 Γ increases linearly with σ_{sf}, and from Figure 1c that at given p and σ_{sf} Γ increases linearly with r_0^2. These results suggest a relationship of $\Gamma \approx \sigma_{sf} r_0^2/p$. Through a number of calculations, we find that this relationship is applicable for all the cases of nonadsorbing surfaces under the salt-free condition. Furthermore, it is also applicable for repulsive and weakly attractive surfaces under the salt-free condition. In all these cases, electrostatic interaction dominates, and it is the competition between the electrostatic attraction of the particle surface and PEs and the electrostatic repulsion among the PE segments that determines the PE adsorption.

dx.doi.org/10.1021/ma201632p |Macromolecules 2011, 44, 8607–8613

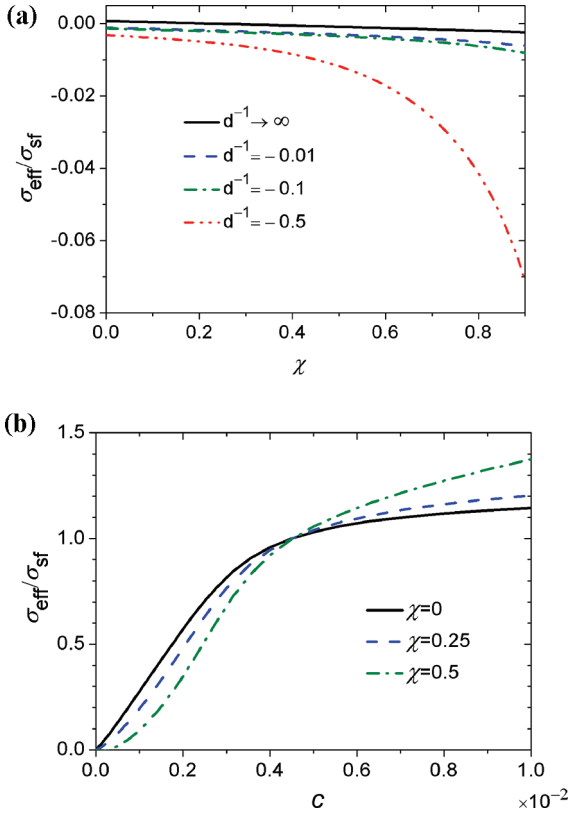

Figure 4. (a) Effect of solvent quality χ on the charge inversion ratio σ_{eff}/σ_{sf} for $c = 0$, $\sigma_{sf} = 0.01$, $p = 0.1$, $\phi_{pb} = 1.25 \times 10^{-4}$, and $r_0 = 10$. (b) Effect of bulk salt concentration c on the charge inversion ratio σ_{eff}/σ_{sf} for a nonadsorbing surface with $\sigma_{sf} = 0.01$, $p = 0.1$, $\phi_{pb} = 1.25 \times 10^{-4}$, and $r_0 = 10$.

When all other parameters are fixed, there is a critical radius r_c, above which PEs are absorbed and below which PEs are depleted from the surface. A plot of r_c vs c is shown in Figure 2 for the nonadsorbing surface in a good solvent ($\chi = 0$). It is noted that, when c is small, r_c is small, increases slowly with increasing c, and is almost independent of ϕ_{pb}; that is, at low salt concentrations, adsorption occurs even for small particles, and the crossover between adsorption and desorption is almost independent of ϕ_{pb}. When c is large, r_c increases sharply with increasing c, indicating that desorption occurs at high enough salt concentrations. Moreover, the adsorption−desorption crossover here depends on ϕ_{pb}; that is, at a given c value, r_c is smaller when ϕ_{pb} is lower. The critical lines shown in Figure 2 are quite similar to those found in SCF calculations for cylindrical surfaces.[25]

The critical surface charge density σ_c is a useful experimental quantity.[8] When $\sigma_{sf} > \sigma_c$, PEs are adsorbed onto the surface, whereas they are depleted when $\sigma_{sf} < \sigma_c$. Furthermore, one may write $c \sim \sigma_c^b$, which has been found experimentally for the system of PEs and oppositely charged micelles.[26] Figure 3 shows c as a function of σ_c for the case of nonadsorbing surface in a good solvent ($\chi = 0$), from which we obtain via linear fitting $b = 1.034 \pm 0.005$, 0.965 ± 0.004, 0.768 ± 0.004, and 0.726 ± 0.004 for particles with $r_0 = 0.5$, 1, 10, and the planar surface, respectively. It is therefore clear that b decreases with decreasing surface curvature. With the inverse Debye screening length $\kappa = (2c/\varepsilon)^{1/2}$, our results give $\sigma_c \sim \kappa^\nu$, where $\nu = 2/b = 1.93-2.75$. Our ν-values are consistent with the experimentally obtained value of about 2 for PE−micelle systems.[27] In addition, using SCF theory (without GSDA but for a finite chain length $N = 200$), Man et al.[25] predicted $\nu_{cylinder} = 2.3$ for a nonadsorbing cylindrical surface of a large curvature (i.e., $r_0 = 0.5$), which is larger than our ν-value for a spherical surface of the same radius; our results and theirs together seem to support the experimental conclusion of Feng et al. that $\nu_{sphere} < \nu_{cylinder}$ for the spherical and the cylindrical surfaces of the same radius.[26] Finally, we can see from Figure 3 that, at given c, a smaller particle has a larger σ_c value.

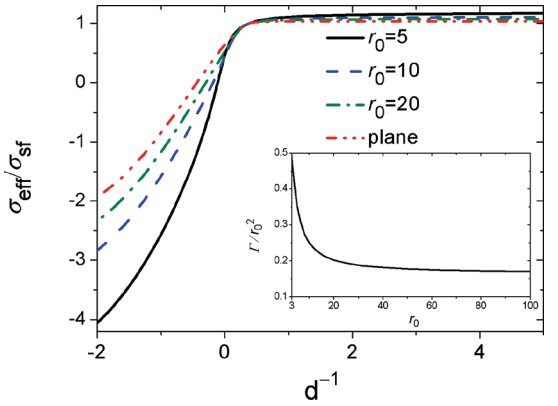

Figure 5. Effect of d^{-1} on the charge inversion ratio σ_{eff}/σ_{sf} for $\sigma_{sf} = 0.015$, $c = 0.015$, $p = 0.1$, $\phi_{pb} = 1.25 \times 10^{-4}$, and $\chi = 0$. The inset shows the r_0-dependence of Γ/r_0^2 with $d^{-1} = -0.5$.

The above results show that PE adsorption may easily occur at low salt concentrations in the case of nonadsorbing surfaces. However, the surface charge inversion does not occur so easily. Figure 4a shows the effect of solvent quality χ on the charge inversion ratio σ_{eff}/σ_{sf} under the salt-free condition, from which we see that a nonadsorbing surface cannot induce strong charge inversion even in a poor solvent. In addition, even an attractive surface with $d^{-1} = -0.5$ can only lead to slight charge inversion in a poor solvent. This is because, as found in the case of planar surfaces studied in ref 9, in the salt-free solution the electrostatic interactions dominate, and the short-range interaction parameters such as χ and d^{-1} have little effects on Γ and σ_{eff}/σ_{sf}. On the other hand, combining the relationship of $\Gamma \approx \sigma_{sf} r_0^2/p$ obtained above with eq 6, we conclude that $\sigma_{eff}/\sigma_{sf} \approx 0$ in the salt-free solution, which is consistent with Figure 4a. Therefore, in the salt-free solution, $\sigma_{eff} \approx 0$ and strong charge inversion by PEs adsorbed onto an oppositely charged spherical surface cannot occur.

Figure 4b shows the effect of bulk salt concentration c on σ_{eff}/σ_{sf} for a nonadsorbing surface. We again see that $\sigma_{eff} \approx 0$ at $c = 0$ regardless of χ. More importantly, σ_{eff}/σ_{sf} increases with increasing c and becomes larger than 1 at high enough c values (say, 0.005), indicating that PEs are depleted from the surface (see eq 6). This is because, at high bulk salt concentrations, electrostatic interactions are largely screened and PEs are thus depleted by the short-range repulsion from the nonadsorbing surface. We therefore conclude that strong charge inversion by PEs adsorbed onto an oppositely charged spherical surface cannot occur for nonadsorbing surfaces. In order to obtain strong charge inversion, we turn to attractive surfaces.

3.2. Attractive Surfaces. Figure 5 shows the effect of d^{-1} on the charge inversion ratio σ_{eff}/σ_{sf} in a good solvent ($\chi = 0$) at a relatively high salt concentration. We see that a strongly attractive surface leads to strong charge inversion. It is also noted that,

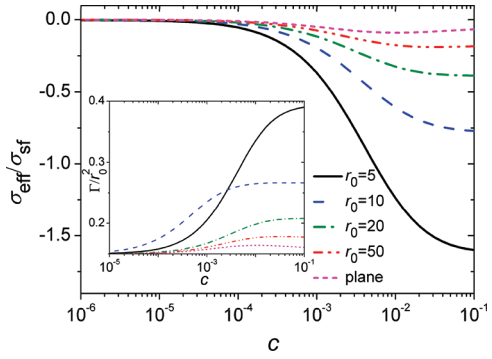

Figure 6. Effect of bulk salt concentration c on the charge inversion ratio σ_{eff}/σ_{sf} and the amount of adsorbed PEs Γ (inset) for an attractive surface ($d^{-1} = -0.5$) with $\sigma_{sf} = 0.015$, $p = 0.1$, $\phi_{pb} = 1.25 \times 10^{-4}$, and $\chi = 0$.

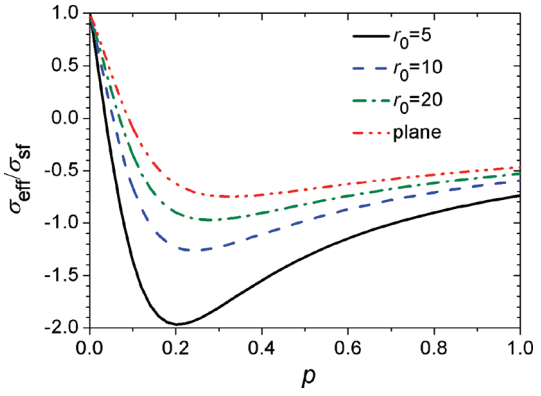

Figure 7. Effect of PE charge fraction p on the charge inversion ratio σ_{eff}/σ_{sf} for an attractive surface ($d^{-1} = -0.5$) with $\sigma_{sf} = 0.015$, $\chi = 0$, $\phi_{pb} = 1.25 \times 10^{-4}$, and $c = 0.015$.

when $d^{-1} < 0$, surface with a smaller radius leads to stronger charge inversion and is more sensitive to the parameter (d^{-1} in this case) variation; this is found in all the cases shown hereafter. Γ/r_0^2 increases with decreasing r_0, which can be seen from the inset of Figure 5; that is, the amount of adsorbed PEs per surface area is larger for a surface with smaller r_0. The charge inversion ratio $\sigma_{eff}/\sigma_{sf} = 1 - p\Gamma/(\sigma_{sf}r_0^2)$ therefore decreases with decreasing r_0. Hereafter, we set $d^{-1} = -0.5$ and examine the effects of various parameters on the surface charge inversion.

Figure 6 shows the effect of c on σ_{eff}/σ_{sf} for an attractive surface in a good solvent ($\chi = 0$). We see that $\sigma_{eff} \approx 0$ at small enough c regardless of r_0, which is consistent with Figure 4b in the salt-free case and indicates that charge inversion by PEs adsorbed onto an oppositely charged spherical surface cannot occur at low salt concentrations even for attractive surfaces. At higher bulk salt concentration, we see that particles with larger curvatures give stronger surface charge inversion. Furthermore, σ_{eff}/σ_{sf} exhibits a minimum for large r_0 (at $c = 0.01$ for the planar surface and at $c = 0.032$ for the $r_0 = 50$ case), due to the competition between the attractive PE−surface electrostatic interaction and the repulsive segment−segment electrostatic interaction. For smaller r_0, the attractive PE−surface electrostatic interaction is weaker due to the smaller surface area, and the repulsive segment−segment electrostatic interaction becomes dominant; σ_{eff}/σ_{sf} therefore decreases monotonically with increasing c (for $c < 0.1$). The inset of Figure 6 shows the

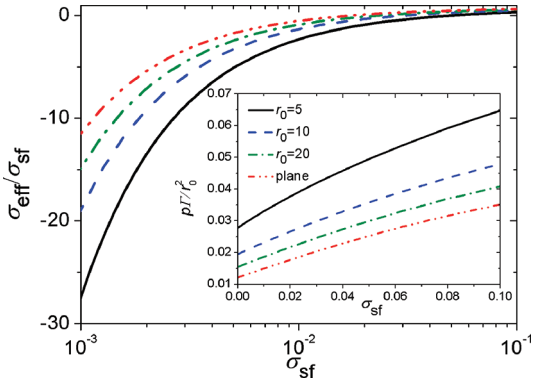

Figure 8. Effect of surface charge density σ_{sf} on the charge inversion ratio σ_{eff}/σ_{sf} for an attractive surface ($d^{-1} = -0.5$) with $p = 0.1$, $\phi_{pb} = 1.25 \times 10^{-4}$, $\chi = 0$, and $c = 0.015$. The inset shows the σ_{sf}-dependence of $p\Gamma/r_0^2$ (for the planar surface case, the vertical axis of the inset denotes $p\gamma$ with γ being the amount of adsorbed PEs per surface area).

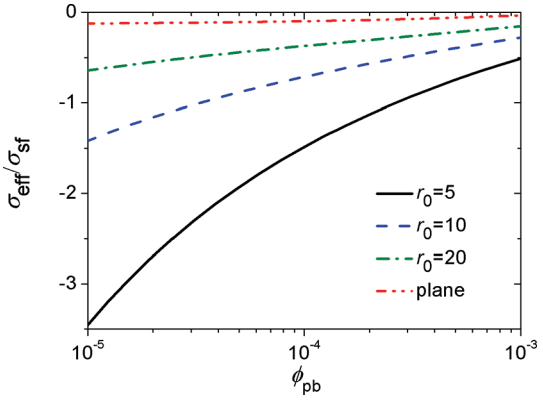

Figure 9. Effect of bulk PE segmental density ϕ_{pb} on the charge inversion ratio σ_{eff}/σ_{sf} for an attractive surface ($d^{-1} = -0.5$) with $p = 0.1$, $\sigma_{sf} = 0.05$, $\chi = 0$, and $c = 0.001$.

corresponding effect of c on Γ, where we see that for large r_0 Γ exhibits a maximum in accordance to the minimum of σ_{eff}/σ_{sf}. A similar maximum in Γ was observed in the experimental study of Shubin et al. on the adsorption of a low linear charge density cationic polyacrylamide onto monodisperse silica particles.[28]

Figure 7 shows the effect of PE charge fraction p on σ_{eff}/σ_{sf} for an attractive surface in a good solvent ($\chi = 0$). We see that all the curves exhibit a minimum around $p = 0.2$. This is because with increasing p the dominant interaction in the system changes from the surface−PE electrostatic attraction to the segment−segment electrostatic repulsion; the former leads to the increase of Γ (i.e., the decrease of σ_{eff}/σ_{sf}) while the latter leads to the decrease of Γ with increasing p. Similar behavior was also found in ref 9 for an indifferent planar surface ($d^{-1} = 0$) in Θ solvent.

Figure 8 shows the effect of surface charge density σ_{sf} on σ_{eff}/σ_{sf} for an attractive surface in a good solvent ($\chi = 0$). We see that σ_{eff}/σ_{sf} increases with increasing σ_{sf}. It is interesting to see that very strong charge inversion occurs for surfaces with low σ_{sf}. While the increase of σ_{sf} enhances the PE−surface electrostatic attraction and leads to an increase in Γ, the inset of Figure 8 shows that the latter is slower than the former; Γ/σ_{sf} therefore decreases with increasing σ_{sf}, which results in the increase of σ_{eff}/σ_{sf} with increasing σ_{sf}.

dx.doi.org/10.1021/ma201632p |*Macromolecules* 2011, 44, 8607–8613

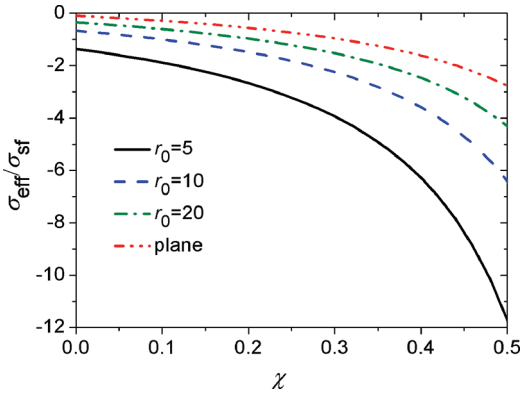

Figure 10. Effect of solvent quality χ on the charge inversion ratio σ_{eff}/σ_{sf} for an attractive surface ($d^{-1} = -0.5$) with $\sigma_{sf} = 0.015$, $p = 0.1$, $\phi_{pb} = 1.25 \times 10^{-4}$, and $c = 0.015$.

Figure 9 shows the effect of the bulk PE segmental density ϕ_{pb} on σ_{eff}/σ_{sf} for an attractive surface in a good solvent ($\chi = 0$). We see that a lower bulk PE segmental density gives stronger charge inversion. This was also found in ref 9 for an indifferent planar surface in Θ solvent.

Finally, Figure 10 shows the effect of solvent quality χ on σ_{eff}/σ_{sf} for an attractive surface. It is noted that σ_{eff}/σ_{sf} decreases with increasing χ. This is reasonable considering that the poor solvent condition can create an effective attraction between PEs and the surface. Similar results were found for nonadsorbing ($d^{-1} \rightarrow \infty$) and indifferent ($d^{-1} = 0$) planar surfaces[9] and for an attractive ($d^{-1} = -0.5$) cylindrical surface.[29] We note that a strong charge inversion ratio of $\sigma_{eff}/\sigma_{sf} = -11.7$ is obtained at $\chi = 0.5$ for a spherical surface with $r_0 = 5$.

4. CONCLUSIONS

In this work, we numerically solve the continuum self-consistent field equations under the ground-state dominance approximation to study the adsorption and charge inversion of flexible polyelectrolytes (PEs) on oppositely charged spherical surfaces. The effects of various parameters on the amount of adsorbed PEs (Γ) and the surface charge inversion ratio (σ_{eff}/σ_{sf}) are examined, including the particle radius (r_0) and its surface charge density (σ_{sf}), the PE charge fraction (p), the short-range surface−PE interactions (d^{-1}), solvent quality (χ), and bulk PE concentration (ϕ_{pb}) and salt concentration (c).

It is found that, when the electrostatic interactions dominate in the system, a relationship of $\Gamma \approx \sigma_{sf} r_0^2/p$ is generally satisfied. For nonadsorbing surfaces (where $d^{-1} \rightarrow \infty$), variation of the critical radius r_c with c is obtained at different values of ϕ_{pb}. We found that r_c is smaller when ϕ_{pb} is lower. Regarding the critical surface charge density σ_c, a scaling relationship of $c \sim \sigma_c^{\ b}$ is obtained, and the value of b decreases with increasing r_0. It is found that strong charge inversion does not occur in a salt-free solution or on a nonadsorbing surface.

For attractive surfaces ($d^{-1} < 0$), particles with smaller r_0 lead to stronger charge inversion because the amount of adsorbed PEs per surface area is larger than in the case of particles with larger r_0. Stronger surface−PE short-range interaction (i.e., decreasing d^{-1}) also leads to stronger charge inversion. Because added salt screens the electrostatic repulsion among PE segments, strong charge inversion occurs at high salt concentrations when r_0 is small enough. With increasing p, the dominant interaction in the system changes from the surface−PE electrostatic attraction to the electrostatic repulsion among PE segments, and σ_{eff}/σ_{sf} exhibits a minimum as p varies from 0 to 1. Increasing σ_{sf} enhances the surface−PE electrostatic attraction and leads to an increase in Γ, which is however slower than the increase of σ_{sf}; smaller σ_{sf} therefore leads to stronger charge inversion. The poor solvent condition creates an effective attraction between PEs and the surface; larger χ therefore leads to stronger charge inversion. Finally, a lower ϕ_{pb} gives stronger charge inversion. Our results on the charge inversion are consistent with previous SCF calculations for planar[9] and cylindrical[29] surfaces.

We consider here a finite bulk PE concentration (i.e., $\phi_{pb} = 10^{-5}-10^{-3}$), which is more relevant to experiments than the previous analytical work[8,10−14] using $\phi_{pb} = 0$. This also makes our definition of the critical condition for PE adsorption different from (thus not directly comparable to) the previous work.[8,10−14] On the other hand, while our work provides predictions that can be qualitatively tested by experiments, quantitative comparisons are often difficult, particularly on the mapping of our short-range interaction parameters (d^{-1} and χ) to experimental systems. In addition, our work has the following limitations: First, we only consider flexible and infinitely long PE chains. Second, the volume and non-Coulombic interactions of small ions are ignored. Third, the dielectric constant is assumed to be the same everywhere in the system. Finally, the correlations and fluctuations in the system are ignored. How to improve these treatments and go beyond the mean-field theory used here will be the topics of our future work.

AUTHOR INFORMATION

Corresponding Author

*E-mail: baohui@nankai.edu.cn (B.L.); q.wang@colostate.edu (Q.W.).

ACKNOWLEDGMENT

This research is supported by the National Natural Science Foundation of China (Grants 20774052 and 20990234), by the National Science Fund for Distinguished Young Scholars of China (No. 20925414), and by Nankai Institute of Scientific Computing. Acknowledgment is also made to the donors of The American Chemical Society Petroleum Research Fund for partial support of this research.

REFERENCES

(1) Wågberga, L.; Wintera, L.; Ödberga, L.; Lindströma, T. *Colloids Surf.* **1987**, *27*, 163–173.
(2) Napper, D. H. *Polymeric Stabilization of Colloidal Dispersions*; Academic Press: New York, 1983.
(3) Hara, M. *Polyelectrolytes: Sciences and Technology*; Dekker: New York, 1993.
(4) Finch, C. A. *Industrial Water Soluble Polymers*; The Royal Society of Chemistry: Cambridge, 1996.
(5) Alberts, B.; Bray, D.; Lewis, J.; Raff, M.; Roberts, K.; Waltsoi, J. D. *Mol. Biol. Cell*; Garland: New York, 1994.
(6) Dubin, P.; Bock, J.; Davis, R.; N., S. D.; Thies, C. *Macromolecular Complexes in Chemistry and Biology*; Springer-Verlag: Berlin, 1994.
(7) Volkeisteii, M. V. *Molecular Biophysics*; Academic Press: New York, 1977.
(8) Winkler, R. G.; Cherstvy, A. G. *Phys. Rev. Lett.* **2006**, *96*, 066103.
(9) Wang, Q. *Macromolecules* **2005**, *38*, 8911–8922.

(10) von Goeler, F.; Muthukumar, M. *J. Chem. Phys.* **1994**, *100*, 7796–7803.
(11) Haronska, P.; Vilgis, T. A.; Grottenmuller, R.; Schmidt, M. *Macromol. Theory Simul.* **1998**, *7*, 241–247.
(12) Cherstvy, A. G.; Winkler, R. G. *J. Chem. Phys.* **2006**, *125*, 064904.
(13) Winkler, R. G.; Cherstvy, A. G. *J. Phys. Chem. B* **2007**, *111*, 8486–8493.
(14) Cherstvy, A. G.; Winkler, R. G. *Phys. Chem. Chem. Phys.* **2011**, *13*, 11686–11693.
(15) Gurovitch, E.; Sens, P. *Phys. Rev. Lett.* **1999**, *82*, 339–342.
(16) Golestanian, R. *Phys. Rev. Lett.* **1999**, *83*, 2473–2473.
(17) Allen, R. J.; Warren, P. B. *Europhys. Lett.* **2003**, *64*, 468–474.
(18) Allen, R. J.; Warren, P. B. *Langmuir* **2004**, *20*, 1997–2009.
(19) Shi, A.-C.; Noolandi, J. *Macromol. Theory Simul* **1999**, *8*, 214–229.
(20) Wang, Q.; Taniguichi, T.; Fredrickson, G. H. *J. Phys. Chem. B* **2004**, *108*, 6733–6744.
(21) Wang, Q.; Taniguichi, T.; Fredrickson, G. H. *J. Phys. Chem. B* **2005**, *109*, 9855–9856.
(22) Chervanyov, A. I.; Heinrich, G. *J. Chem. Phys.* **2009**, *131*, 104905.
(23) Press, W. H.; Teukolsky, S. A.; Vetterling, W. T.; Flannery, B. P. *Numerical Recipes in Fortran 77: The Art of Scientific Computing*, 2nd ed.; Cambridge University Press: Cambridge, UK, 2002.
(24) Shafir, A.; Andelman, D.; Netz, R. R. *J. Chem. Phys.* **2003**, *119*, 2355–2362.
(25) Man, X. K.; Yang, S.; Yan, D. D.; Shi, A.-C. *Macromolecules* **2008**, *41*, 5451–5456.
(26) Feng, X. H.; Dubin, P. L.; Zhang, H. W.; Kirton, G. F.; Bahadur, P.; Parotte, J. *Macromolecules* **2001**, *34*, 6373–6379.
(27) Cooper, C. L.; Goulding, A.; Basak Kayitmazer, A.; Ulrich, S.; Stoll, S.; Turksen, S.; Yusa, S.; Kumar, A.; Dubin, P. L. *Biomacromolecules* **2006**, *7*, 1025–1035.
(28) Shubin, V. *J. Colloid Interface Sci.* **1997**, *191*, 372–377.
(29) Man, X. K.; Yan, D. D. *Macromolecules* **2010**, *43*, 2582–2588.